Atomic transition probability measurements for spectral lines of the $3s$-$4p$ transition array of neutral carbon

Douglas W. Jones and W. L. Wiese
Atomic and Plasma Radiation Division, National Bureau of Standards, Washington, D.C. 20234
(Received 28 November 1983)

Absolute transition probabilities for the 18 transitions of the $3s$-$4p$ transition array of neutral carbon have been studied in emission with a wall-stabilized arc. Values are given for ten individual lines and one pair of strongly blended lines (476.23 and 476.25 nm). An upper bound is set for the remaining six lines of the array which were too weak to be observed in this work. An important feature of this work is the use of digital least-squares-fitting techniques to separate overlapping lines and to provide accurate line-wing corrections. Problems associated with demixing effects have been avoided by normalizing relative transition probability measurements to an absolute scale set by atomic lifetimes.

INTRODUCTION

Many of the prominent lines in the visible spectrum of neutral carbon belong to the $3s$-$4p$ transition array. The determination of atomic transition probabilities for spectral lines of this transition array has been therefore the objective of numerous experimental[1–9] and theoretical[10–12] endeavors published over the course of the past 30 years. All the experimental work has been done in emission spectroscopy and, with the exception of the shock-tube work by Miller *et al.*,[3] all experimenters have used various forms of the wall-stabilized arc[13] as the emission source. Despite the similarities in these experiments there has been substantial disagreement among the results. This is probably largely due to three problem areas: (a) the difficulty in determining precisely the number density of carbon atoms in the observed region of the source for absolute transition probability determinations; (b) the problem of determining individual line strengths for overlapping lines in the $3s$-$4p$ triplet multiplets; and (c) the treatment of line-wing contributions for multiplet spectra and low-resolution spectra of lines with different widths. The new measurements presented in this work were undertaken because solutions for each of these problems are now available. In the following, the history of the three critical areas is reviewed in some detail, and the techniques employed in this work to avoid these problems are outlined.

(a) Absolute transition probability determination. With respect to this factor, since carbon is most easily introduced into the source as a constituent of a molecular gas (CO_2, CH_4, CH_3SH, C_2H_5OH), and often this gas is mixed with another gas such as argon, demixing becomes a serious problem.[14] Prior to about 1963 all the published results for carbon transition probabilities were calculated using nominal gas mixture ratios and assuming no demixing. A critical compilation of atomic transition probabilities, the U.S. National Bureau of Standards (NBS) tables of 1966,[15] tried to compensate for demixing by rescaling the existing measurements to agree with an absolute scale based on theoretical values generated by the Coulomb approximation.[16] Uncertainties in the range of 50% were assigned to the resulting values for the $3s$-$4p$ transition array of neutral carbon.

Since the publication of the NBS tables[15] several approaches to the demixing problem have been tried. Foster[4] chose to normalize his relative data to the value given in the NBS tables[15] for the 505.22-nm spectral line of the $3s$-$4p$ transition array and thus incorporated the uncertainty of the tabulated value (50%) into his absolute scale. Employing a shock tube as the emission source, Miller *et al.*[3] assume that nominal gas mixture ratios are valid on the grounds that demixing cannot occur on the short time scale of the shock heating. The shock-tube data, however, were recorded on photographic plates and suffer from the inherent uncertainties in analyzing photographic data and from the inevitable integration of temperatures and densities over the duration of the pulsed emission. Goly[1] has applied a diagnostic technique which allows the determination of number densities of atomic species in the observed region of his arc source. Unfortunately, this technique relies heavily on the theory of Stark broadening for nonhydrogenic lines,[17] and gives transition probability results which are very sensitive to uncertainties in the temperature determination. In the case of the results given by Goly[1] the contributions to the transition probability uncertainties from the number density and temperature determinations are 10% and 20%, respectively.

At the present time it appears that the most accurate absolute transition probabilities are obtained by normalizing relative transition probabilities to an absolute scale determined from atomic lifetime measurements. This approach eliminates the demixing problem by making the determination of number densities unnecessary, and it vastly reduces the contribution of uncertainties in the temperature determination to the overall uncertainties of the transition probability results. Precise lifetime data for some neutral carbon levels are now available, and Stuck and Wende[2] have already used this method to determine transition probabilities for several lines in the far-ultraviolet spectrum of neutral carbon and for the 505.22-nm line of the $3s$-$4p$ transition array. This method has also been used in the work reported in this paper:

Relative transition probabilities have been measured for the individual spectral lines of the $3s$-$4p$ transition array, and these measurements have been normalized to the absolute scale determined by the transition probability of the 505.22-nm line which follows from the work of Stuck and Wende.[2]

(b) Individual line strengths for overlapping lines. A second significant problem in determining transition probabilities for individual lines of the $3s$-$4p$ transition array of neutral carbon arises from line blending. Under the plasma conditions of a wall-stabilized arc operating near local thermodynamic equilibrium (LTE) all the transitions between the $3s$ and $4p$ triplet levels appear as multiplets of overlapping and blended lines. For this reason all the experimental work prior to 1966 reported only transition probabilities for entire multiplets. The NBS compilation[15] lists transition probabilities for individual lines of these multiplets which have been obtained from the overall multiplet values by applying theoretical line strength ratios based on the *LS*-coupling scheme. Some values for individual lines of these multiplets have been published in the more recent works,[1,3] but only for lines which did not appear to overlap too severely; in both cases the results are based on more or less qualitative judgements of the effects of the wings of adjacent lines. In this paper digital data processing techniques have been employed to address this problem. The individual lines are extracted from the raw data by applying digital least-squares-fitting techniques[18] to spectral scans which provide precise profiles of the blended multiplets. This procedure generates individual line radiances for all the lines of the $3s$-$4p$ transition array which could be observed in this work except for two lines (476.23 and 476.25 nm) which were too strongly blended to be resolved by this technique.

(c) Line-wing contributions. The intensity contributions of the extended line wings also can be taken into account properly by these digital techniques. Since the spectral scans in this work provide precise information on the actual shapes of the spectral radiance profiles, the least-squares-fitting technique yields analytical curves which approximate each of the observed line shapes. This provides two possible approaches to the problem of determining accurate line-wing corrections: either the area under the untruncated analytical curve may be used to obtain the total line radiance, or only the wings of the analytical curve may be used to provide line-wing corrections to a numerical integration of the actual data points. Either of these approaches should be much more accurate than corrections based on visual estimates of the number of half-widths included in an area measured by manual planimetry, a method commonly employed in the past. In the case of several overlapping lines in a blended multiplet the use of some form of fitted analytical curve appears to be the only means of accurately correcting for truncated line-wings.

EXPERIMENTAL METHOD

The emission source used in this work was a wall-stabilized arc,[13] 88 mm long, consisting of a stack of 5-mm-thick water-cooled copper plates separated by 1.2-mm-thick insulating spacers and with a 4.2-mm central bore diameter. Argon gas flowed into the arc from both ends and surrounded the tungsten electrodes. The working gas was introduced at the midpoint of the arc. All the gases exited the arc chamber through exhaust openings near both of the electrodes but still within the constrictive bore of the arc. By properly adjusting the flow rates of the gases the working gas could be restricted to a well-defined cylindrical volume while maintaining atmospheric pressure within the arc channel. The radiation from the arc was observed end-on through uv-grade fused-silica windows approximately 3 mm thick. These windows were tilted a few degrees from being perpendicular to the arc axis and wedged about three-quarters of a degree to prevent distortion of the data by spurious reflections and interference effects.

For most of the measurements the working gas was a mixture of about 84 vol% carbon dioxide in argon, but pure carbon dioxide gas and a mixture of about 10 vol% carbon dioxide in argon were also used occasionally. In all cases a small amount (on the order of 0.1 vol%) of hydrogen gas was added to the working gas for plasma diagnostic purposes. In the course of these experiments it was found that the amount of hydrogen introduced into the arc had to be kept quite small to retard the production of water vapor by hydrogen-oxygen combustion in the cooler regions of the arc chamber. The water produced by this chemical reaction tended to condense on the cooled copper arc plates and eventually sputter back into the arc channel causing noticeable instabilities in the emission from the arc.

The radiation from the arc was imaged onto the entrance slit of a 2.25-m Czerny-Turner monochromator by a concave mirror. The mirror was positioned to magnify the image of the arc bore by about 2.3 times. A rectangular diaphragm limited the effective aperture of the collection optics to about $f/80$, and the entrance slit of the monochromator was masked to a height of 0.6 mm so that only a narrow region along the central axis of the arc was observed. A laser directed into the exit slit of the monochromator was used to align the optical system by retracing the entire optical path. The monochromator was equipped with an 1800 line/mm holographic grating yielding a linear dispersion of about 0.24 nm/mm. For measurements of the arc radiation both the entrance and exit slits were set at 22.5 μm to produce an instrument-limited linewidth of about 0.005 nm. A photomultiplier tube with a broadband GaAs photocathode and a uv-transmitting glass envelope served as the detector. The photomultiplier was cooled to -30°C in order to reduce its dark current and to improve its stability. The thermoelectric photomultiplier cooler has a vacuum insulated window composed of two 1.5-mm-thick uv-grade fused-silica plates which were wedged and tilted by about the same amounts as the arc windows. The photoelectric signals were amplified, filtered to eliminate high-frequency noise, and converted to a voltage signal with a range of 0—10 V.

A minicomputer performed on line-recording of the photoelectric signals and controlled the scanning unit of the monochromator. At each position in a spectral scan

the computer recorded the wavelength setting of the monochromator and then paused for 1 s to allow the photomultiplier signal to stabilize. When this "settling time" had passed the computer digitally averaged the photoelectric signal for a 5-s period by sampling the signal 500 times at 0.01-s intervals with a 12-bit analog-to-digital converter. Once the computer had computed and recorded the average signal, it commanded the scanning unit to advance the monochromator by a wavelength increment of 0.02 nm and then repeated the data-acquisition process. The line profiles recorded by the computer in these stepwise scans were subsequently corrected for minor dark current variations and calibrated against the measured spectral response of the detection system. In this manner precise absolute spectral radiance profiles were generated for each of the multiplets studied in this work.

In order to test for possible self-absorption effects a concave mirror was placed behind the arc so that it imaged the arc back into itself. A mechanical shutter actuated by the computer was placed between this mirror and the arc and successive wavelength points were recorded with the shutter alternately open or closed. Scanning a profile in this fashion acquires, in effect, two profiles simultaneously: one of the arc plasma itself and one of the sum of the plasma and its reflected image. These profiles establish the degree of self-absorption at each wavelength position in a spectral scan and pointwise corrections can be made by the computer which result in a reconstruction of the line profiles as they would appear in the absence of self-absorption. The computer algorithm[18] developed for this purpose has been thoroughly tested and proven to be effective in studies of actual self-absorbed data[19] and in computer simulations of self-absorption where the "true" profile is known. The digital technique employed here is more sensitive to self-absorption effects and more accurate than the method of merely checking for a constant ratio of alternating points across a line profile. Self-absorption studies were performed when the working gas was pure carbon dioxide, and the measured degree of self-absorption was found to be insignificant by comparison to the normally observed statistical scatter of the data. A further test involved a tenfold change in the nominal carbon dioxide concentration (10 vol% vs 100 vol%) which did not indicate any systematic trend in the data as might be expected if appreciable self-absorption were present at the higher concentrations. These results established that the arc emitted as an optically thin source throughout this work. Also, it should be noted that the least-squares-fitting technique described below tends to compensate for minor amounts of self-absorption. This follows from the fact that small amounts of self-absorption will only have an appreciable effect on relatively few points near the center of the line while the least-squares fit includes many points in the wings of the lines where self-absorption falls off rapidly.

The absolute spectral calibration of the detection system was carried out with two tungsten strip lamps. One lamp was used as a transfer standard which was scanned at the end of each data run to provide the absolute spectral response of the detection system to be used in calibrating that set of data. The other lamp is a sparsely used reference standard calibrated by the Radiometric Physics Division at the National Bureau of Standards whose calibration is periodically transfered to the working lamp. Calibration transfers are performed by placing the reference standard lamp in the position normally occupied by the arc and with all intermediate optical elements including the arc window still in place and comparing sequential scans of this lamp and the working transfer standard lamp. The relatively low radiance of the tungsten strip lamps made it necessary to increase the exit slits of the monochromator to 90.0 μm for all calibration transfers. Only the exit slits were altered from the conditions used in acquiring data from the arc. It was observed that this fourfold increase in the exit slit width did not merely increase the photoelectric signals by a factor of 4, but rather displayed a slight wavelength dependence which is in qualitative agreement with the increased diffraction losses of the narrower slits at longer wavelengths. Careful measurements of this effect showed that the slit correction factor could be approximated well by a linear function of wavelength which ranged from about 4.44 at 538 nm to about 4.39 at 477 nm for the work presented here. Scans of the transfer standard lamp from each of the data runs were also compared to one another at the end of these experiments to ensure the consistency of the ratio of the calibration scans. This final test of the calibration accuracy yielded minor corrections ($<1\%$ in nearly all cases) to the relative transition probability values.

Plasma diagnostics to determine the temperature of the arc plasma were performed by measuring the Stark width of H_β. This is the well-established technique[13,17] whereby the calculated dependence of the Stark width on electron density[20] is used first to obtain the electron density. Once the electron density is known the temperature is determined by solving the LTE and conservation equations[21] for a plasma of the appropriate composition with the aid of tabulated partition functions.[22] In the work that is presented here the plasma was assumed to have the composition given by the nominal gas mixture ratios and demixing was ignored in determining the temperature. Although this procedure introduces a significant systematic uncertainty of about 200 K into the temperature determination, it has a very small effect on the relative transition probability results. The propagated uncertainty due to the estimated indeterminacy in the temperature contributes less than 0.4% to the uncertainties of the relative transition probabilities because the excitation energies of the upper levels involved in this work lie within a range of less than 1700 cm^{-1}.

As measured by the above technique, arc plasma temperatures were varied over the range of 11 350 to 12 230 K in the course of the present work. Corresponding electron densities ranged from 8.25×10^{16} to 6.56×10^{16} cm^{-3}. Arc currents of 45, 55, and 60 A were used with the different gas mixtures discussed above to obtain this range of plasma conditions.

ANALYSIS PROCEDURES

A major objective of the work presented here has been the determination of accurate transition probabilities for

individual lines of multiplets which appear typically as overlapping or blended lines. The method employed for this purpose applies digital least-squares-fitting techniques to the measured spectra to obtain analytical "synthetic" spectra. Implementation of such a technique requires both the functional form which approximates the observed line shapes and one which approximates the background radiation pedestal that underlies the line spectra. In the plasma environment of an arc operating near LTE at atmospheric pressure the dominant line-broadening process is Stark broadening by electron collisions. Thus, the observed line profiles were assumed to be approximately Lorentzian.[17] This assumption has been tested continuously throughout this work and previous studies,[19,23] and the Lorentzian line shape has proven to be an excellent approximation to the observed line shapes of Stark-broadened lines. The choice of a functional form which approximates the background radiation pedestal is somewhat more arbitrary. Over the limited wavelength range of a single spectral scan (<5 nm) the background radiation is typically composed of continuum radiation and the wings of spectral lines which lie outside the range of the scan. This generates a smooth, slowly varying background which may in some cases have a modest degree of curvature. Empirical tests showed that a cubic polynomial approximation to the background radiation pedestal provided a reasonable compromise between analytical simplicity and good approximation. Again, the validity of the assumed functional form was monitored continuously in this work.

Each synthetic spectrum employed in this work consisted of a single Lorentzian profile for each line observed in the corresponding scan data and a cubic polynomial background function. The sum of these components provided an analytical composite curve for each spectrum which was made to match the actual data points of a spectral scan by digital least-squares fitting. The major difficulty in this technique arises from the nonlinear dependence of Lorentzian profiles on the position and width parameters. This necessitates the use of an iterative fitting procedure. In order for this type of fit to converge on the best possible values, carefully chosen initial values of the nonlinear parameters must be supplied as the starting point for the iteration. Initial values were provided in this work by a computer program[18] which examines spectral scan data for possible spectral lines and makes relatively crude estimates of the position, height, and width of each line it locates. Occasionally these values were manually adjusted to reduce the time required by the iterative fit which followed. The program which performs the actual least-squares fit employs a two-stage iteration procedure.[18] In the first stage the nonlinear parameters remain fixed and least-squares values for the linear parameters are calculated by a multiple linear regression routine.[24] The linear parameters in this stage are the four coefficients of the cubic polynomial and the areas under the Lorentzian profiles. The linear parameters from the first stage remain fixed in the second stage where least-squares values are found for the nonlinear parameters (peak position and half-width) by an adaptation of the iterative gradient-expansion algorithm given by Bevington.[24,25] At the completion of the second stage the entire two-stage process is repeated and this continues until the variance of the fitted curve from data points is being reduced by less than 0.01% on successive iterations. This two-stage iterative procedure is faster and requires less computer memory than merely applying the iterative gradient-expansion algorithm to determine all the linear and nonlinear parameters simultaneously.

A typical example of the analysis procedure described above is illustrated in Fig. 1 which shows the central portion of the most complicated spectra studied in this work. The points surrounded by open squares in the figure are the spectral radiance data points from the arc measurements. The solid line is the analytical curve of the synthetic spectrum. In this case the synthetic spectrum is composed of the sum of five individual Lorentzian profiles and a cubic background radiation pedestal. The analytical curves of the individual components are indicated by the dashed lines. Clearly, the fitted synthetic spectrum provides a reasonable approximation to the observed spectrum; the calculated standard deviation of the composite fitted curve from the actual data points is less than 0.4% of the vertical scale shown in Fig. 1. Note the separation of the weak line at 477.00 nm from its blend with the much stronger 477.17-nm line. A limitation of this procedure is illustrated by the lines at 476.23 and 476.25 nm, however. These two lines are too severely blended to be resolved by this technique and have been fitted to a single Lorentzian profile. For clarity, the vertical axis in Fig. 1 has been offset to eliminate most of the background radiation, and it should be noted that the wavelength scale in the figure is shifted slightly by an offset in the wavelength calibration of the monochromator.

The synthetic spectra provided two values for the integrated spectral radiance of each spectral line. One value resulted from the area under the fitted analytical curve; the other from numerical integration of the residue which remained when the fitted curves of all competing spectral components were subtracted from the measured data points. Line-wing corrections to the numerically integrated values were provided by the analytical line wings. The degree of agreement between these two values provides one test of the validity of the assumptions which go into the fitting procedure. In all cases corresponding values of the total line radiances agreed with each other to better than 0.1%. As an additional test, the standard deviation of each fitted curve from its corresponding data points was calculated for each of the 51 spectral scans analyzed in this work and was found to be acceptably small with values ranging from 0.16% to 1.4%. The fitting procedure also proved to be relatively insensitive to minor deviations of the actual line shapes from the idealized Lorentzian profiles. As mentioned above the fit tends to compensate for small amounts of self-absorption, and small deviations resulting from slight asymmetries in the observed line shapes[26] were found to cancel one another almost completely.

During each run of the experiment the composition and temperature of the plasma were held constant while various $3s$-$4p$ multiplets of the neutral carbon spectrum were

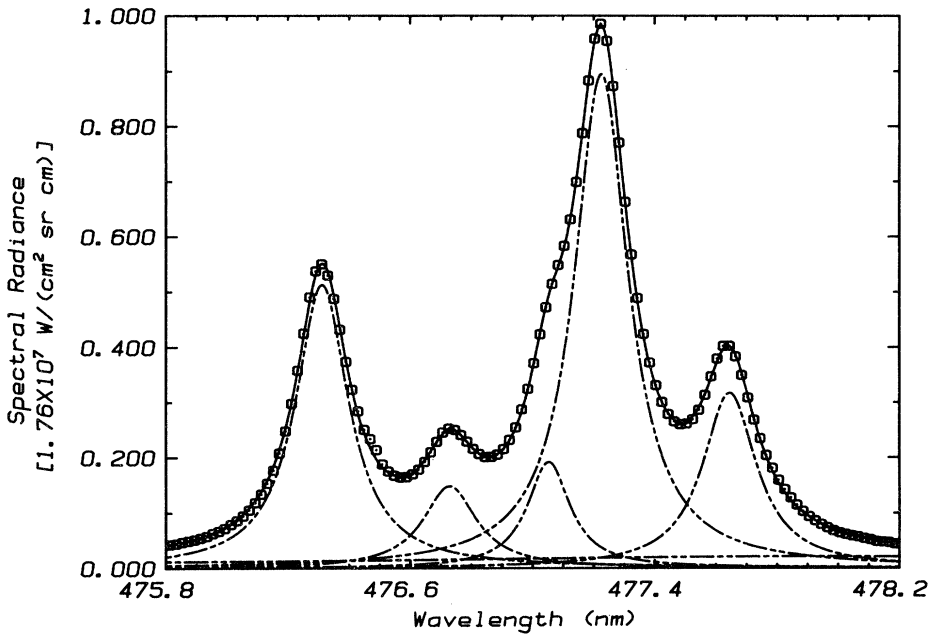

FIG. 1. A portion of one of the spectral scans of the neutral carbon lines in the $3s$-$4p$ transition array illustrating the overlap of six Stark-broadened lines. Points surrounded by open squares are the actual data points; the smooth curves are the analytical results of the digital least-squares-fitting technique described in the text. Peak at the far left corresponds to a pair of strongly blended spectral lines, 476.23 and 476.25 nm, which have been fitted to a single Lorentzian profile because they could not be separated by this technique. Continuing from left to right, the remaining spectral lines are located at 476.67, 477.00, 477.17, and 477.59 nm. The six dashed curves are the five Lorentzian profiles and the nearly flat background radiation polynomial resulting from the least-squares fit; the solid curve is the composite synthetic spectrum obtained by summing together these six components. For clarity the vertical axis has been offset to eliminate most of the continuum background; the horizontal axis is shifted slightly by an offset in the wavelength calibration of the monochromator.

scanned repeatedly. The spectral line at 505.22 nm was measured in every run and served as the reference line for the relative transition probabilities reported here. At the end of each run the total radiance of each line was obtained by calculating the weighted average of values from individual scans. (Statistical weights were assigned on the basis of the goodness-of-fit parameters for both the overall fit and the individual spectral component being considered.) Relative transition probability results for each run were then computed from the average radiance values by means of the expression[19]

$$\frac{A_x}{A_r}=\frac{I_x}{I_R}\frac{\lambda_x}{\lambda_R}\frac{g_R}{g_x}\exp\left[\frac{E_x-E_R}{kT}\right], \tag{1}$$

where the subscripts x and R denote values associated with the line under consideration and the reference line, respectively, and where A represents the corresponding transition probability, I the total line radiance, λ the wavelength, E the excitation energy of the upper level and g its statistical weight, k the Boltzmann constant, and T the temperature. In separate runs with varying plasma conditions, four independent measurements of each relative transition probability were obtained and then combined in a final weighted average. The uncertainty associated with each relative transition probability was estimated by combining the weighted standard deviations, the random uncertainty due to the temperature determination ($<0.4\%$), and the random uncertainty due to the calibration procedures (1%) as Gaussian random errors, and then increasing this statistical uncertainty by an additional 1% to account for estimated systematic errors which might result from the temperature determination (0.4%) and self-absorption (0.6%).

RESULTS AND DISCUSSION

Relative transition probabilities, as determined by the procedures described above, are presented in the third column of Table I. The wavelengths and transition designations in the first two columns of this table are from the multiplet tables compiled by Moore.[27] The remaining columns of Table I list relative transition probabilities derived from past experimental[1,3,4,6–9,15] and theoretical[10–12] studies. (The measurements of Henning[5] are omitted because they do not include the 505.22-nm line which serves as the reference line in Table I; the measurements of Stuck and Wende[2] are also omitted because they include only the 505.22-nm line from $3s$-$4p$ array.) The experimental studies disagree significantly on an absolute scale, so only relative transition probabilities are compared here. The relative values listed in the table were obtained by normalizing the absolute transition probabilities of each study to the transition probability that study quotes for the 505.22-nm line. As noted above, the strongly blended lines at 476.23 and 476.25 nm could not be separated in this work so a combined value for the pair is given in the table. Miller *et al.*[3] give a combined value for this pair, too, and for the pair of lines at 477.00 and 477.17 nm. The weak lines of the multiplet at 489.09 nm

TABLE I. Comparison of relative transition probabilities. Values in parentheses are multiplet-sum values.

Wavelength (nm)	Transition	This work (arc plasma)	Goly Ref. 1 (arc plasma)	Miller *et al.* Ref. 3 (shock tube)	Foster Ref. 4 (arc plasma)	NBS tables Ref. 15 (crit. comp.)	Foster Ref. 6 (arc plasma)	Foster Ref. 7 (arc plasma)	Richter Ref. 8 (arc plasma)	Maecker Ref. 9 (arc plasma)	Hofsaess Ref. 10 (theory)	McEachran and Cohen, Ref. 11 (theory)	Cohen and McEachran Ref. 12 (theory)
476.23	$3s\ ^3P^o_0$–$4p\ ^3P_1$	0.162±3%		0.31		0.31							
476.25	$3s\ ^3P^o_1$–$4p\ ^3P_2$					0.22							
476.67	$3s\ ^3P^o_1$–$4p\ ^3P_1$	0.128±5%		0.30		0.23							
477.00	$3s\ ^3P^o_1$–$4p\ ^3P_0$	0.436±18%		0.63		0.88							
477.17	$3s\ ^3P^o_2$–$4p\ ^3P_2$	0.458±3%				0.71							
477.59	$3s\ ^3P^o_2$–$4p\ ^3P_1$	0.275±4%		0.42		0.36							
(476.97)	$3s\ ^3P^o$–$4p\ ^3P$	(0.581±2%)	(0.563)	(0.94)		(0.91)	(0.783)	(0.75)	(0.92)	(0.60)	(1.6)	(0.50)	(1.2)
481.29	$3s\ ^3P^o_0$–$4p\ ^3S_1$	0.0240±11%	0.040	<0.02		0.057							
481.74	$3s\ ^3P^o_1$–$4p\ ^3S_1$	0.0662±4%	0.056	0.04		0.16							
482.68	$3s\ ^3P^o_2$–$4p\ ^3S_1$	0.0469±4%	0.060	0.063		0.28							
(482.21)	$3s\ ^3P^o$–$4p\ ^3S$	(0.137±3%)	(0.156)	(<0.123)		(0.50)		(0.27)			(1.2)	(0.73)	
488.89	$3s\ ^3P^o_0$–$4p\ ^3D_1$	<0.003											
488.89	$3s\ ^3P^o_1$–$4p\ ^3D_2$	<0.002											
489.06	$3s\ ^3P^o_2$–$4p\ ^3D_3$	<0.001											
489.34	$3s\ ^3P^o_1$–$4p\ ^3D_1$	<0.003											
489.86	$3s\ ^3P^o_2$–$4p\ ^3D_2$	<0.002											
490.31	$3s\ ^3P^o_2$–$4p\ ^3D_1$	<0.003											
(489.09)	$3s\ ^3P^o$–$4p\ ^3D$	(<0.004)									(1.2)	(< 0.005)	
493.20	$3s\ ^1P^o_1$–$4p\ ^1S_0$	2.36±6%	2.35	2.24	2.6	2.7	2.88	2.68	2.7	1.7	0.88	1.89	4.6
505.22	$3s\ ^1P^o_1$–$4p\ ^1D_2$	1.000	1.000	1.000	1.000	1.000	1.000	1.000	1.000	1.000	1.000	1.000	1.000
538.03	$3s\ ^1P^o_1$–$4p\ ^1P_1$	0.663±3%		0.97	0.88	0.94	0.745	0.906	0.96	0.83	0.98	0.240	3.6

could not be observed in this work and only an upper bound on the relative transition probability of each line is given in Table I. Each upper bound is calculated for a hypothetical line radiance of one-tenth the radiance of the weakest line which was observed in this work. Assuming that these lines have widths which are similar to the other lines in the $3s$-$4p$ array, this procedure should provide a valid upper bound. It should be noted that this weak multiplet was not assigned to the $3s$-$4p$ array prior to 1966, and that the wavelength 490.31 nm is a predicted value.[27]

The relative transition probabilities measured in this work agree reasonably well with those derived from Goly[1] and from Miller *et al.*[3] This is particularly true for the multiplet values since errors in separating overlapping lines will tend to cancel when the multiplet sum is determined. Also, there appears to be good agreement among the experiments for the 493.20-nm line. For most of the remaining lines, however, the other experimental and theoretical studies disagree significantly with one another and with this work. The individual line values given by the NBS compilation[15] were obtained by applying line-strength ratios from the *LS*-coupling scheme to data from Foster[7] and from Richter[8] after those data had been renormalized to agree with theoretical results from the Coulomb approximation.[16] The resulting absolute transition probabilites were assigned uncertainties of 50%, but substantial disagreements with the experimental studies since the publication of this compilation suggest that these uncertainties may be overly optimistic for the lines of the triplet multiplet at 482.21 nm on even a relative scale. Of the three theoretical studies included in the table the polarized frozen-core (PFC) calculation of McEachran and Cohen[11] appears to provide the best overall agreement with the experiments.

The uncertainty associated with each relative transition probability measured in this work is also listed in the third column of Table I. As discussed above, these uncertainties include estimates of systematic errors, random uncertainties, and statistical standard deviations encountered in the determination of each value. In most cases the major contribution to the overall uncertainties comes from the statistical scatter of the data from different scans and from different runs of the experiment. This scatter appears to be an indication of slowly varying drifts, i.e., extremely low-frequency noise in either the emission of the arc or the response of the detection system. The predominant contributions to the two largest uncertainties of 18% for the 477.00-nm line and 11% for the 481.29-nm line are statistical and appear to be largely due to the difficulty of separating these weak lines from overlapping stronger lines at 477.17 and 481.74 nm, respectively.

Absolute transition probabilities have been obtained from the relative measurements listed in the second column of Table I by normalizing these results to an absolute scale based on the work of Stuck and Wende.[2] By first measuring the transition probability of the longest-wavelength resonance multiplet of neutral carbon (165.7 nm) relative to the 505.22-nm line of the $3s$-$4p$ array and then normalizing this result to the lifetime measurement of Lawrence and Savage[28] for the upper level of the resonance transitions, Stuck and Wende made an accurate determination of the absolute transition probability for the 505.22-nm line.[2] In order to obtain a somewhat more accurate normalization for the data presented in this work a slight modification of their procedure has been followed. The modified procedure employs two of the three relative transition probabilities which may be derived from the study by Stuck and Wende,[2] and two of the lifetimes from the measurements of Lawrence and Savage.[28] These quantitites are combined to yield two values for the normalization factor which are averaged to obtain a normalization factor that should be more reliable than one based on a single lifetime and a single relative transition probability. Table II lists the values which were used to implement this procedure. The last column of this table lists the two values of the normalization factor A_R (in effect, the transition probability of the reference line) which follow from the other values in the table by means of the expression

$$A_R = \left[t_k \sum_i \frac{A_{ki}}{A_R} \right]^{-1}, \tag{2}$$

where A_{ki}/A_R is the relative transition probability for the transition from the upper atomic energy level k to lower level i, and t_k is the lifetime of the upper level; the summation is over all the spontaneous emission transitions originating from the upper level. The normalization factors in Table II have an average value of 1.49×10^6 s^{-1} with a net uncertainty of 12%. The uncertainty in this factor and for the two values shown in the table have been obtained by assuming independent random uncertainties with normal distributions. If, instead, the uncertainties are assumed to be entirely systematic, then the net uncertainty in the normalization factor becomes 22%. Stuck and Wende have made the latter assumption in estimating the uncertainties in this study.[2] The average normalization factor used here establishes an absolute scale which is about 5% lower than the one which was used by Stuck and Wende.[2]

TABLE II. Values used in obtaining the absolute normalization factor.

Wavelength (nm)	g_k	$g_k A_{ki}$ (10^8 s^{-1})	A_{ki}/A_R	t_k (ns)	A_R (10^6 s^{-1})
165.7	9	29[a]	206±12%[a]	3.1±10%[b]	1.57±16%
193.09	3	11[a]	234±12%[c]	2.9±10%[b]	1.40±16%
247.86		0.54[a]	11.5±12%[c]		

[a]Value directly from Ref. 2.
[b]Value directly from Ref. 28.
[c]Value derived from Ref. 2.

Table III lists the absolute transition probabilities which are obtained when the relative transition probabilities in Table I are multiplied by the average normalization factor discussed above. As in Table I, the wavelengths and transition designations in the first two columns of this table are from the multiplet tables by Moore.[27] The third column of Table III lists the absolute transition probability results and the estimated uncertainty associated with each value. Once again, the uncertainties have been estimated by assuming independent, random, normally distributed individual contributions, i.e., by calculating the square root of the sum of the squared contributions to the net uncertainty. Based on the nature of the contributions involved here, this method appears to provide the most reasonable estimates[24] of the overall uncertainties. The uncertainties which follow from the assumption of entirely systematic errors may be obtained by simply adding 22% to each of the uncertainties shown in Table I.

In summary, it has been shown that digital data processing techniques are essential for the accurate determination of individual atomic transition probabilities for overlapping spectral lines. By applying these techniques, relative transition probabilities for ten prominent lines in the visible spectrum of neutral carbon have been precisely measured. Also, an upper bound has been determined for the relative transition probabilities of six very weak lines of the $3s$-$4p$ transition array of this spectrum, and a combined relative transition probability for two very strongly blended lines of this array has been obtained. These relative results have been normalized to an absolute scale determined by recent lifetime measurements.

TABLE III. Absolute transition probabilities for neutral carbon from this work. Values in parentheses are multiplet-sum values.

Wavelength (nm)	Transition	A_{ki} (10^6 s^{-1})
476.23	$3s\ ^3P^o_0$–$4p\ ^3P_1$	0.241±12%
476.25	$3s\ ^3P^o_1$–$4p\ ^3P_2$	
476.67	$3s\ ^3P^o_1$–$4p\ ^3P_1$	0.190±13%
477.00	$3s\ ^3P^o_1$–$4p\ ^3P_0$	0.648±22%
477.17	$3s\ ^3P^o_2$–$4p\ ^3P_2$	0.680±12%
477.59	$3s\ ^3P^o_2$–$4p\ ^3P_1$	0.408±13%
(476.97)	$3s\ ^3P^o$–$4p\ ^3P$	(0.863±12%)
481.29	$3s\ ^3P^o_0$–$4p\ ^3S_1$	0.0357±16%
481.74	$3s\ ^3P^o_1$–$4p\ ^3S_1$	0.0983±13%
482.68	$3s\ ^3P^o_2$–$4p\ ^3S_1$	0.0697±13%
(482.21)	$3s\ ^3P^o$–$4p\ ^3S$	(0.204 ±12%)
488.89	$3s\ ^3P^o_0$–$4p\ ^3D_1$	<0.005
488.89	$3s\ ^3P^o_1$–$4p\ ^3D_2$	<0.003
489.06	$3s\ ^3P^o_2$–$4p\ ^3D_3$	<0.002
489.34	$3s\ ^3P^o_1$–$4p\ ^3D_1$	<0.005
489.86	$3s\ ^3P^o_2$–$4p\ ^3D_2$	<0.003
490.31	$3s\ ^3P^o_2$–$4p\ ^3D_1$	<0.005
(489.09)	$3s\ ^3P^o$–$4p\ ^3D$	(<0.006)
493.20	$3s\ ^1P^o_1$–$4p\ ^1S_0$	3.51±13%
505.22	$3s\ ^1P^o_1$–$4p\ ^1D_2$	1.49±12%
538.03	$3s\ ^1P^o_1$–$4p\ ^1P_1$	0.985±12%

[1]A. Goly, Astron. Astrophys. 52, 43 (1976).
[2]D. Stuck and B. Wende, Phys. Rev. A 9, 1 (1974).
[3]M. H. Miller, T. D. Wilkerson, R. A. Roig, and R. D. Bengston, Phys. Rev. A 9, 2312 (1974).
[4]E. W. Foster, J. Phys. B 3, L145 (1970).
[5]H. Henning, Z. Astrophys. 62, 109 (1965).
[6]E. W. Foster, Proc. Phys. Soc. London 79, 94 (1962).
[7]E. W. Foster, Proc. Phys. Soc. London, Sec. A 80, 882 (1962).
[8]J. Richter, J. Phys. 151, 114 (1958).
[9]H. Maecker, Z. Phys. 135, 13 (1953).
[10]D. Hofsaess, J. Quant. Spectrosc. Radiat. Transfer 28, 131 (1982).
[11]R. P. McEachran and M. Cohen, J. Quant. Spectrosc. Radiat. Transfer 27, 119 (1982).
[12]M. Cohen and R. P. McEachran, J. Quant. Spectrosc. Radiat. Transfer 20, 295 (1978).
[13]W. L. Wiese, in *Methods of Experimental Physics,* edited by B. Bederson and W. L. Fite (Academic, New York, 1968), Vol. 7B, pp. 307–353.
[14]J. Richter, Z. Astrophys. 53, 262 (1961); W. Frie and H. Maecker, Z. Phys. 162, 69 (1961).
[15]W. L. Wiese, M. W. Smith, and B. M. Glennon, *Atomic Transition Probabilities,* U.S. Natl. Bur. Stand., Natl. Stand. Ref. Data Ser. No. NSRDS-NBS 4 (U.S. GPO, Washington, D.C., 1966), Vol. 1.
[16]D. R. Bates and A. Damgaard, Philos. Trans. R. Soc. London, Ser. A 242, 101 (1949).
[17]H. R. Griem, *Spectral Line Broadening by Plasmas* (Academic, New York, 1974).
[18]D. W. Jones, computer code SDAAP: *Spectral Data Acquisition and Analysis Program Package* (Natl. Bur. Stand., Washington, D.C., 1983).
[19]K. Musiol, D. W. Jones, and W. L. Wiese, J. Quant. Spectrosc. Radiat. Transfer 29, 321 (1983).
[20]C. R. Vidal, J. Cooper, and E. W. Smith, Astrophys. J. Suppl. Ser. 214 25, 37 (1973).
[21]W. L. Wiese, in *Methods of Experimental Physics,* edited by B. Bederson and W. L. Fite (Academic, New York, 1968), Vol. 7A, pp. 117–141.
[22]W. Drawin and P. Felenbok, *Data for Plasmas in Local Thermodynamics Equilibrium* (Gauthier-Villars, Paris, 1965).
[23]D. W. Jones, K. Musiol, and W. L. Wiese, in *Spectral Line Shapes,* edited by K. Burnett (de Gruyter, Berlin-New York, 1983), Vol. 2, pp. 125–136.
[24]P. R. Bevington, *Data Reduction and Error Analysis for the Physical Sciences* (McGraw-Hill, New York, 1969).
[25]D. W. Marquardt, J. Soc. Ind. Appl. Math. 11, 431 (1963).
[26]D. W. Jones and W. L. Wiese (unpublished).
[27]C. W. Moore, *Selected Tables of Atomic Spectra, Atomic Energy Levels and Multiplet Tables,* C I, C II, C III, C IV, C V, C VI, U.S. Natl. Bur. Stand. Natl. Stand. Ref. Data. Ser. No. NSRDS-NBS 3 (U.S. GPO, Washington, D.C., 1970), Sec. 3.
[28]G. M. Lawrence and B. D. Savage, Phys. Rev. 141, 67 (1966).